

Experimental and Detonation-Shock Dynamics analyses of cellular detonations in diverging channels: the effects of the cross-sectional shape

Vianney Monnier, Vincent Rodriguez, Pierre Vidal, Ratiba Zitoun

Institut Pprime, UPR 3346 CNRS, ENSMA, 86961 Futuroscope-Chasseneuil, France

1 Introduction

The reaction zone of detonations in gases has an inherently 3D cellular structure. We recently demonstrated that the cross-sectional shape of a straight channel significantly influences the cellular patterns if there are not enough cells per unit area on the front of a self-sustained detonation [1, 2]. In this analysis, we focus on channels with round or square cross sections that increase at a moderate linear rate. We analyze the transients of the cellular structure when the detonation front enters the diverging channel from a straight one, based on front-view and side-view of the cell patterns.

In straight channels, the cell patterns on the front views are irregular regardless of the mixture composition and the cross-sectional shape of the channel if the number of cells per unit area is large enough, i.e., if the initial pressure p_0 or cross-sectional area A is large enough. If not, the front-view patterns depend on the shape of the cross-sectional shape. However, the side views show diamond-shaped patterns whose regularity mostly depends on the composition of the mixture [3]. Thus, side views alone may not fully characterize the cellular structure, and the cell dynamics at the walls of a channel may not represent that of the entire detonation front.

The analysis of a sufficiently large number of cells on a side view defines a cell mean width $\bar{\lambda}$, which can be a relevant characteristic length only if the irregularity of the diamonds is not too high: $\bar{\lambda}$ is statistically meaningless if the standard deviation of the widths is comparable to, or larger than, $\bar{\lambda}$. Furthermore, a relevant mean width should be intrinsic, that is, determined solely by the combustion process, which is not the case if there are not enough cells per unit area of the front. When relevant, $\bar{\lambda}$ serves as a parameter of detonation dynamics to quantify detonability. Thus, for self-sustaining propagation, i.e., close to the theoretical Chapman-Jouguet (CJ) upper limit, there should be at least $\mathcal{O}(100)$ cells on the detonation front, i.e., $d/\bar{\lambda} > 10$, where d is the smaller transverse dimension of the channel.

Former analyses for diverging channels with a smoothly increasing cross-sectional area, e.g. [4–13], have focused on the effects of p_0 , composition of the mixture, and the cone half-angle α : increasing p_0 or decreasing α favors the continuity of the cellular structure, and decreasing p_0 or increasing α favors inward-propagating quenching of the chemical reactions and hence the disappearance of the cellular structure. Typically, the detonation behaves as if the area change were abrupt when $\alpha \geq 60^\circ$ [9].

To our knowledge, the effect of cross-sectional shape on smooth transmission in diverging channels has not been previously described, which is what this work addresses using square and round cross-sections. The analysis builds upon our previous investigation for straight channels [1] with the stoichiometric mixture $2\text{H}_2 + \text{O}_2 + 2\text{Ar}$. We had observed that the front-view patterns were irregular and independent of the cross-sectional shape when the cell number was sufficiently large, but the diamonds on the side views remained regular for all p_0 , regardless of shape. For low values of p_0 , the diamonds were thinner, and the front-view patterns more regular in the square tube than in the round one. In the present work, we consider the low value $p_0 = 20$ kPa. We first collect experimental data on the 3D transients of the cellular front during its transmission in the diverging channels, based on soot-coated foil recordings. We then interpret the results using a Detonation-Shock Dynamics relationship linking normal acceleration and velocity, and total curvature of the leading shock [14–16].

2 Experimental methodology and setup

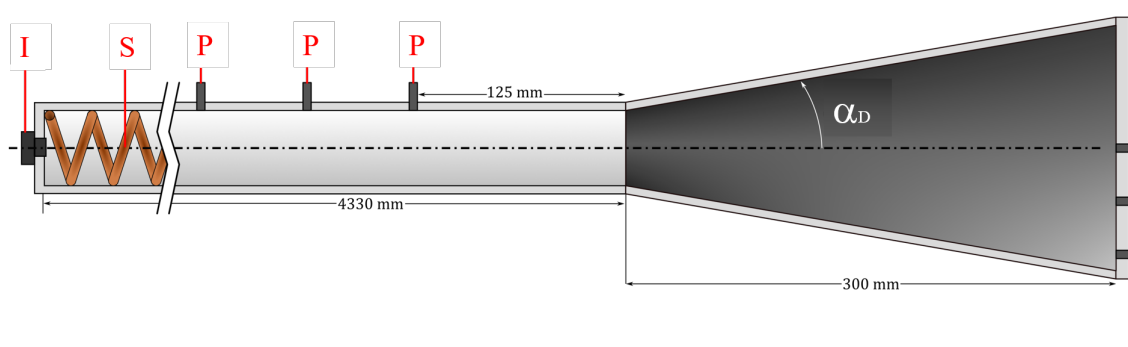


Figure 1: Schematic of the setup. I: ignition, S: Shchelkin spiral, P: pressure transducers.

The experimental setup (Fig. 1) is a diverging channel positioned at one end of a straight tube [1]. The diverging channel has the same shape and initial area as the straight tube ($A_0 = 16 \text{ cm}^2 \pm 4\%$). We used two cross-sectional shapes: one square and the other round, with all other dimensions (e.g., tube length, cross-sectional area) being equal. A spark plug (I) at the end of the straight tube opposite of the diverging channel generated a deflagration, and a Shchelkin spiral (S) ensured transition to detonation at a typical position 1 m relative to the ignition. The linear rate of area increase $d(A/A_0)/dx$ of the cross sections of the diverging channels was the same for the square and round shapes. This ensures the same area $A(x)$ at the same abscissa x relative to the entries of the diverging channels, but implies different constant half-angles α for round and square cross sections, here 9.8° and 8.7° , respectively. The side views of the cellular structure were recorded on soot-coated foils placed along the walls of the straight and diverging channels. The front views were obtained with soot-coated foils placed perpendicular to the propagation direction, at successive abscissas $x \geq 0$ from the entries of the diverging channels, from one experiment to another. Three piezoelectric pressure sensors (Kistler 603B) on the walls of the straight channels were used to obtain an average wave velocity and check its steadiness before the detonation enters the diverging channels. Steadiness was also based on the criterion that the cells should have about constant geometric properties before entering the diverging channels. The mixture $2\text{H}_2 + \text{O}_2 + 2\text{Ar}$ was prepared in a separate tank using the partial-pressure method and then injected at the initial pressure $p_0 = 20 \text{ kPa}$ and the initial temperature $294 \pm 3 \text{ K}$ after vacuuming the tubes.

3 Results

Figure 2 compares recordings in the round and square diverging channels. In our conditions, the small values of the divergence half-angles α ensured continuity of the cellular structure, i.e., the supercritical case of transmission. In the square diverging channel, from $A/A_0 = 1$ to 2, there is no significant effect of the area increase, except for a few squared patterns that are deformed. The initial regularity ($x = 0$, $A/A_0 = 1$) of the front-view patterns essentially persists, and the cell number remains identical to its value at the channel entry. From $A/A_0 = 2$, domains with deformed patterns appear with stochastic distribution and number increasing with A . From $A/A_0 = 4.7$, all front-view patterns have irregular shapes, independent of the wall orientation(s). In the round diverging channel, the front views show irregular cells right from the entry of the diverging channel.

Figure 3 compares cell widths, λ , measured in the diverging channels with square (blue symbols) and round (red symbols) cross sections, as well as in the straight tubes with a 71 cm^2 round section and a 25 cm^2 square section (green symbols). The shape of the symbols represents that of the channel. The cell widths λ are plotted against the dimensionless area $A(x)/A_0$, the higher the color intensity, the larger

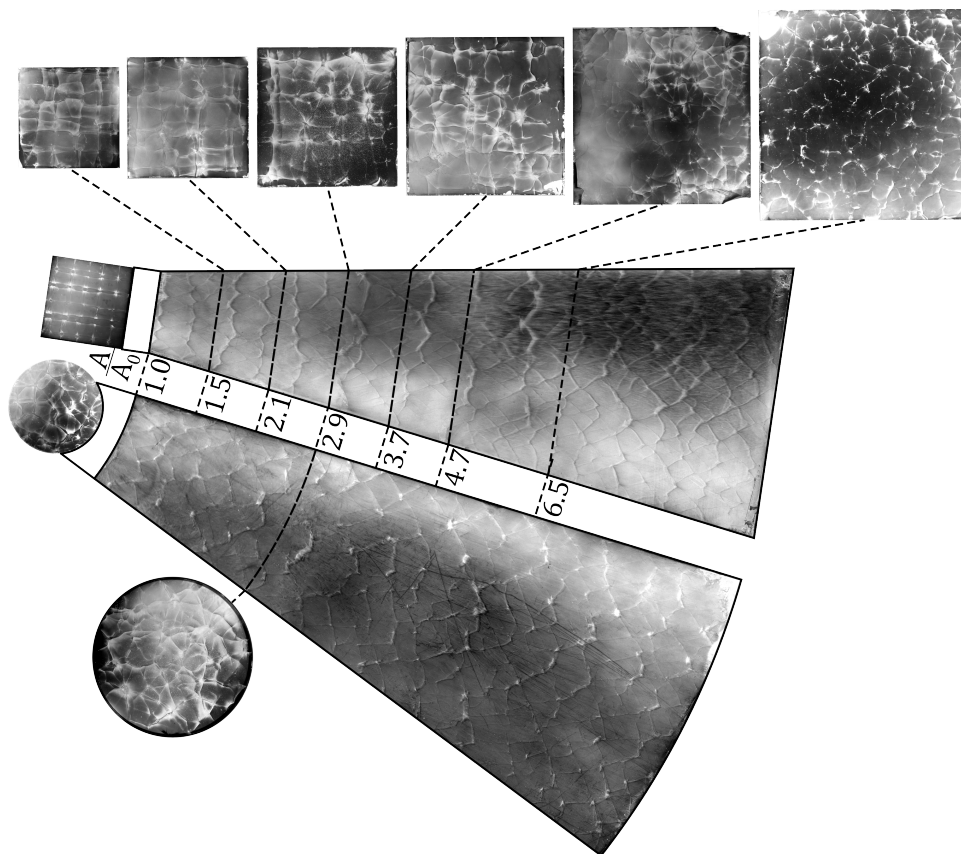


Figure 2: side-view and front-view recordings of detonation cellular structures in the round tube (left) and in the square tube (right). The cross-sectional areas have the same initial value $A_0 = 16 \text{ cm}^2$ and the same rate of increase. Mixture: $2 \text{ H}_2 + \text{O}_2 + 2 \text{ Ar}$. Initial pressure: $p_0 = 20 \text{ kPa}$. Initial temperature: $T_0 = 294 \text{ K}$.

the number of cells with a given width. The blue and red solid lines are the boundaries of the domains comprising 68% of measured widths. The black symbols give the mean cell widths $\bar{\lambda}$ in the diverging channels. They are calculated over abscissa intervals $\Delta x = 30 \text{ mm}$, large enough to include enough cells so that a mean width is significant. Thus, the characteristic displacement time of the wave front between the positions x where A/A_0 and the cell number are measured is larger than the characteristic beat time of the cells, and the axial or transverse variations of the cell number with increasing x or A/A_0 result in nonambiguous changes in the cell width. Regardless of the cross-sectional shape, $\bar{\lambda}$ increases with increasing A/A_0 , before decreasing from $A/A_0 \sim 3$ to stabilize at the same value $\bar{\lambda} \sim 11 \pm 0.5 \text{ mm}$, which is higher than the value of $\sim 9 \text{ mm}$ obtained with the largest straight tube (71 cm^2) where the influence of the section shape would be negligible [1].

The values of $\bar{\lambda}$ are larger, and the position of their maximum is lower, in the round diverging channel. The largest values of $\bar{\lambda}$ are ~ 15 and $\sim 12.5 \text{ mm}$, and their positions correspond to the dimensionless areas A/A_0 of 2.5 and 3, in the round and square channels, respectively. The mean cell width becomes independent of the cross-section shape from the abscissa x where $A/A_0 \sim 6$, consistent with the observation in Figure 2 that irregular patterns then cover the entire front surface.

These trends in front-view recordings and cell widths are essentially the same as would be observed at the same p_0 in straight channels with cross-sectional areas increasing from one experiment to the other, or in the same straight channel with p_0 increasing from one experiment to the other.

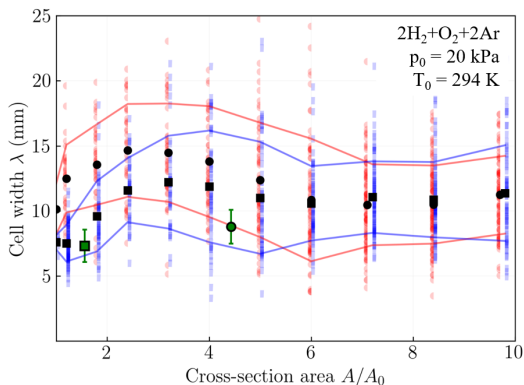


Figure 3: Cell widths λ measured in diverging channels with square and round cross sections (square and round symbols, respectively) whose areas A increase linearly, cf. Sects. 2 and 3.

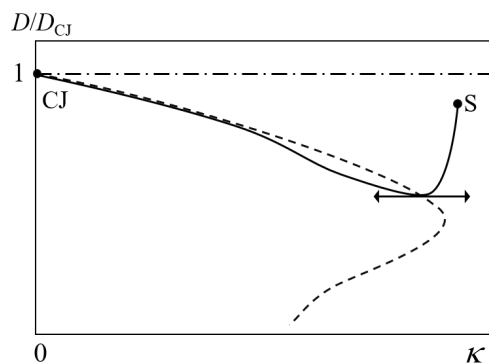


Figure 4: Diffracting detonation dynamics in the Velocity D - Curvature κ plane. Full line: integral curve from the initial condition at point S. Dashed line: 0-acceleration curve.

4 Discussion and conclusion

Gubin and Kogarko [6] conducted a series of experiments in an diverging round cross-section channel connected to a 32 mm diameter straight tube and with an expansion half-angle of 60° or 45° . They observed supercritical transmissions with non-monotonic evolution of the front perturbations (presumably $\sim \lambda$), similar to the trends shown in Figure 3, where the detonation velocity D first decreases before increasing. They noted that these effects became smaller as the initial pressure increased. Our results show that using different cross-sectional shapes at a constant initial pressure leads to similar effects on $\bar{\lambda}$. They also bring out the long relaxation time of $\bar{\lambda}$ after the shape effect has vanished. The analysis below offers a plausible interpretation based on the relation of Detonation Shock Dynamics (DSD) [14–16],

$$\frac{\delta D}{\delta t} = V^2 (W - \kappa), \quad (1)$$

which includes the effects of normal acceleration $\delta D/\delta t$ and total curvature κ on the normal velocity of the detonation leading shock. Relation (1) is valid only for self-sustained detonations. This is the case in this work because the detonation in the straight channel was self-sustained before entering the diverging channels and because of the small values of the divergence half-angles. The term V represents the velocity of a perturbation propagating on the front surface, and V/D is the tangent of the local half-angle α_M of its Mach cone. The term W relates to chemical kinetics. Relation (1) embeds the classical $D - \kappa$ relationship, e.g. [17–19], valid only for very large radii of curvature compared to the characteristic chemical length (the distance from the shock to the sonic locus), i.e., when the acceleration effect is negligible. The simplest expressions for V and W are obtained in the limit of high activation energies of the chemical process and in the approximation of a constant ratio γ of the specific heats [16],

$$V(D) = \sqrt{\frac{2\gamma^2}{4\gamma^2 + \gamma - 3}} \times D, \quad (2)$$

$$W(D) = \frac{\gamma^2 - 1}{8\gamma^2} \left(\left(\frac{D_{CJ}}{D} \right)^2 - 1 \right) \times \frac{1}{\ell(D)}, \quad (3)$$

where $\ell(D)$ is the induction length behind a constant-velocity planar shock. The assumption of large activation energy gives a qualitatively correct description of wave dynamics, but it cannot provide reliable quantitative information.

Typical values of γ are around 1.1 and 1.3, which result in local Mach angles $\alpha_M \simeq 40^\circ$. These values are much larger than the channel expansion angles. Physically, this ensures that the perturbations from the walls influence the wave front dynamics. Mathematically, this makes the problem well-posed, and the relation (1) applicable to the current analysis.

In our conditions, the cell dynamics in the straight channels, i.e., before diffraction, depends on the cross-sectional shapes, so the average shape of the detonation front close to the wall should be considered as only quasi-planar ($\kappa \gtrsim 0$) and its normal velocity close to the CJ value ($D \lesssim D_{CJ}$). Immediately after diffraction, and although small, the sudden transverse expansion of the flow forces this curved part of the front to decelerate, hence the initial condition represented by point S in figure 4. Thus, the initial effect of curvature is necessarily greater than that of energy production, i.e., $\kappa > W$, so $\delta D/\delta t \propto \delta D/\delta R < 0$ from (1). Then, as the wave expands, both the wave velocity and curvature decrease. The curvature effect eventually becomes smaller than that of the chemical production term W , after the integral curve has reached the 0-acceleration $D - \kappa$ curve, and the front decreasingly accelerates up to the CJ point, i.e., $\kappa < W$, so $\delta D/\delta t \propto \delta D/\delta R > 0$. These sequences explain the non-monotonic behavior in Figure 3, as the mean cell width λ increases when the velocity of the average detonation front decreases.

Relation (1) also suggests a plausible explanation for why the cell mean widths are larger in the round cross section at the beginning of the diffraction process and why this difference vanishes as the wave progresses. Geometry shows that the total curvature of a spherical wave is twice that of a cylinder of the same radius. Therefore, the curvatures of the diffracted fronts are necessarily greater in a round cross-section than in a square cross-section, so that the deceleration is greater in the round tube, which results in larger chemical lengths and cells. Equivalently, the rate of increase in cell width is greater in the round diverging channel. As the wave progresses, the deceleration effect disappears, and the only remaining effect is that of the vanishing small expansion. That explains both why the cell widths tend to become asymptotically the same at large values of A/A_0 and why this asymptotic value is larger than in the straight channels of greater areas. The effect of the wave front curvature seems to have a very long characteristic time of disappearance, so that much longer channels are certainly necessary to reach the intrinsic cell width corresponding to the CJ detonation, i.e., the planar wave.

Experiments in a narrow diverging channel with a non-linearly enlarging rectangular cross-section and a high expansion rate are described in [20, 21], and the results could be analyzed with a $D(\kappa)$ DSD modeling, i.e., without acceleration effect. Our experiments in weakly diverging channels with round or square cross-sections show a non-ambiguous non-monotonic variations in cell width at the entries in the enlarging channels (Fig. 3), indicating the need for a modeling that includes the acceleration effect.

In conclusion, this experimental work and its detonation-shock-dynamics interpretation show that the transient dynamics of three-dimensional detonation cells is highly sensitive to small changes in the boundary conditions and that, in particular, it takes a long time for the cellular dynamics to become independent of the geometry of diverging channels. This high sensitivity also makes the data collected in this work a relevant experimental basis for high-resolution numerical simulations capable of handling three-dimensionality and detailed chemical kinetics mechanisms. It emphasizes that the conditions for measuring detonation cell widths require constant cross-section tubes of sufficient size and length.

Acknowledgements

This work was supported by the Ministry of Higher Education, Research and Innovation (France)

References

- [1] Monnier V., Rodriguez V., Vidal P., Zitoun R. (2022). An analysis of three-dimensional patterns of experimental detonation cells. *Comb. and Flame*. 245: 112310. doi.org/10.1016/j.combustflame.2022.112310
- [2] Monnier V., Rodriguez V., Vidal P., Zitoun R. (2023). Three-dimensional dynamics of detonation diffraction: effects of the tube cross-section shape. *Proceedings of the 29th International Colloquium on the Dynamics of Explosions and Reactive Systems*, Paper 059.
- [3] Manzhalei V. I., Mitrofanov V. V., Subbotin V. A. (1974). Measurement of inhomogeneities of a detonation front in gas mixtures at elevated pressures. *Comb. Expl. and Shock Waves* 10: 89-95. doi.org/10.1007/BF01463793
- [4] Kogarko S. M., (1956). On the possibility of detonation of gaseous mixtures in conical tubes. *Izv. Akad. Nauk SSSR, Otd. Khim. Nauk* 4 419–426.
- [5] Gubin S. A., Kogarko S. M., Mikhalkin V. N. (1981). Experimental study of gas detonation in conical tubes. Translated from *Fizika i Vzryva* 18 (1981) 111–117. doi:10.1007/BF00800631
- [6] Gubin S. A., Kogarko S. M., Mikhalkin V. N. (1981). Experimental study of gas detonation in conical tubes. *Explosion and Shock Waves* 18 (1982) 592–597. doi:10.1007/BF00800631
- [7] Strehlow R. A., Salm R. J., The failure of marginal detonations in expanding channels, *Acta Astronautica* 3 (11) (1976) 983–994. doi:10.1016/0094-5765(76)90007-2.
- [8] Thomas G., Edwards D. H., Lee J. H., Knystautas R., Moen I. O., Wei Y. M., Detonation diffraction by divergent channels, in: *Dynamics of Explosions*, J.-C. Leyer and R.I. Soloukhin and J.R. Bowen, 1986, pp. 144–154. doi:10.2514/5.9781600865800.0144.0154.
- [9] Borisov A., Khomik S. V., Sanevt E. V., Critical energy of direct detonation initiation in gaseous mixtures, in: *Dynamics of Detonations and Explosions: Detonations*, Vol. 133, AIAA, 1989, pp. 142–155. doi:10.2514/5.9781600866067.0142.0155.
- [10] Guilly V., Khasainov B., Presles H. N., Desbordes D., Influence de la dilution par l'argon d'un mélange C₂H₂ / O₂ sur les conditions critiques de diffraction de sa détonation, *Mécanique et industrie* 196 (2005) 269–273. doi:10.1051/meca:2005028.
- [11] Khasainov B., Presles H.-N., Desbordes D., Demontis P., Vidal P., Detonation diffraction from circular tubes to cones, *Shock Waves* 14 (2005) 187–192. doi:10.1007/s00193-005-0262-9
- [12] Sorin R., Zitoun R., Khasainov B., Desbordes D., Detonation diffraction through different geometries, *Shock Waves* 19 (2009) 11–23. doi:10.1007/s00193-008-0178-1.
- [13] Endo T., Kobayashi R., Kuwajima S., Seki Y., Kim W., Johzaki T., Detonation propagation from a cylindrical tube into a diverging cone, *Journal of Thermal Science and Technology* 15 (2020). doi:10.1299/jtst.2020jtst0030
- [14] Brun L., Une théorie de la détonation dans les explosifs condensés fondée sur l'hypothèse de Jouguet (1989), Rapport CEA/DAM DPM/BS 224/89
- [15] Kasimov A., Stewart D., Asymptotic theory of evolution and failure of self-sustained detonations, *J. Fluid Mech.* 525 (2005) 161–192. doi:10.1017/S0022112004002599.
- [16] Vidal P., Critical slow dynamics of detonation in a gas with non-uniform initial temperature and composition: a large activation-energy analysis, *International Journal of Spray and Combustion Dynamics (IJSCD)* 1(2) (2009) 435–471. doi:10.1260/175682709789685822.
- [17] Wood, W. W. and Kirkwood, J. G., Diameter effect in condensed explosives. The relation between velocity and radius of curvature of the detonation wave, *J. Chem. Phys.* 2(11), 1920-1924 (1954). doi.org/10.1063/1.1739940
- [18] Bdzil, J. B. and Stewart, D. S., Theory of Detonation Shock Dynamics, In: Zhang, F. (eds) *Shock Waves Science and Technology Library*, Vol. 6. Shock Wave Science and Technology Reference Library, vol 6. Springer, Berlin, Heidelberg. (2012) doi.org/10.1007/978-3-642-22967-1-7
- [19] Short, M. and Voelkel, S. J. and Chiquete, C., Steady detonation propagation in thin channels with strong confinement, *J. Fluid Mech.* 889, (2020). doi.org/10.1017/jfm.2020.37
- [20] Xiao Q. and Radulescu M., Dynamics of hydrogen–oxygen–argon cellular detonations with a constant mean lateral strain rate, *Comb. Flame* 215, (2020) 437-457. doi.org/10.1016/j.combustflame.2020.01.041
- [21] Radulescu M. and Borzou B., Dynamics of detonations with a constant mean flow divergence, *J. Fluid Mech.* 845, (2018) 346–377. doi.org/10.1017/jfm.2018.244